Ab-initio chemical potentials of solid and liquid solutions and the chemistry of the Earth's core

D. Alfè[⋆†], M. J. Gillan[†] and G. D. Price[⋆]

[⋆]Geological Sciences Department, University College London
Gower Street, London WC1E 6BT, UK

[†]Physics and Astronomy Department, University College London
Gower Street, London WC1E 6BT, UK

Abstract

A general set of methods is presented for calculating chemical potentials in solid and liquid mixtures using *ab initio* techniques based on density functional theory (DFT). The methods are designed to give an *ab initio* approach to treating chemical equilibrium between coexisting solid and liquid solutions, and particularly the partitioning ratio of solutes between such solutions. For the liquid phase, the methods are based on the general technique of thermodynamic integration, applied to calculate the change of free energy associated with the continuous interconversion of solvent and solute atoms, the required thermal averages being computed by DFT molecular dynamics simulation. For the solid phase, free energies and hence chemical potentials are obtained using DFT calculation of vibrational frequencies of systems containing substitutional solute atoms, with anharmonic contributions calculated, where needed, by thermodynamic integration. The practical use of the methods is illustrated by applying them to study chemical equilibrium between the outer liquid and inner solid parts of the Earth's core, modelled as solutions of S, Si and O in Fe. The calculations place strong constraints on the chemical composition of the core, and allow an estimate of the temperature at the inner-core/outer-core boundary.

1 Introduction

We present here a set of techniques that allow the *ab initio* calculation of chemical potentials in solid and liquid solutions, and hence the *ab initio* treatment of chemical equilibrium between solid and liquid phases. There are many areas of chemical physics where such techniques might be important, but we believe they have a particular role to play in studying the partitioning of impurities between different phases under extreme conditions, where experiments are difficult or impossible. As an illustration of the power of the techniques, we will describe how we have applied them to study chemical equilibrium between the solid and liquid parts of the Earth's core.

The techniques to be presented form a natural sequel to recent developments in the *ab initio* thermodynamics of condensed matter based on electronic density-functional theory (DFT) [1]. For many years, DFT has been used to calculate the phonon spectra of perfect crystals [2], and it is only a short step from that to the calculation of free energies and other thermodynamic quantities in the harmonic approximation. There have already been several reports of DFT calculations of high-temperature crystal thermodynamics [3, 4, 5, 6, 7, 8, 9], including solid-solid phase equilibria [10, 11, 12, 13] using this approach. For liquids, *ab initio* thermodynamics first became possible with the Car-Parrinello technique [14] of DFT molecular dynamics simulation, which immediately gave a way to calculate such quantities as pressure, internal energy and temperature of a liquid in thermal equilibrium. The first DFT treatment

of solid-liquid equilibrium was achieved by Sugino and Car [15], who used thermodynamic integration to compute the free energies of solid and liquid Si, and hence the melting properties of the material. Closely related is the work of de Wijs *et al.* [16] on the melting of Al. We have recently reported DFT calculations of the free energies and melting curves of Fe [9, 17, 18] and Al [19] over a wide range of pressures; Jesson and Madden [20] have recently presented *ab initio* calculations of the zero-pressure melting properties of Al using their 'orbital free' approach. The work of Smargiassi and Car [21] and Smargiassi and Madden [22] on the free energy of formation of defects in crystals is also relevant to the ideas to be presented here.

Thermodynamic integration has been the key to calculating the *ab initio* free energy of liquids and anharmonic solids, and hence to the treatment of solid-liquid equilibrium. It provides a means of computing the difference of free energy between the *ab initio* system and a reference model system whose free energy is known. We will show that it is also the key to calculating *ab initio* chemical potentials of liquids and anharmonic solids, but here it is used in a rather different way. The chemical potential of a species is the free energy change when an atom of that species is added to the system. The difference of chemical potentials of two species is therefore the free energy change when an atom of one species is replaced by an atom of the other, or equivalently when one atom is transmuted into the other. The role of thermodynamic integration here is to provide a way of calculating the free energy change associated with such transmutations, and we shall show how this can be accomplished in practical DFT simulations. This general approach is closely related to ideas that have been used for a long time in classical simulation. A recent example of classical thermodynamic integration with molecular transmutation to calculate solvation free energies in aqueous solution can be found in Ref. [23], which gives references to earlier literature.

Although the techniques we shall present are fairly general, we do impose two restrictions at present: First, the theoretical framework is developed for the case of a two-component mixture; second, one of the components is present at low, but not very low, concentration, in a sense to be clarified in Sec. 2. The situation envisaged therefore consists of fairly dilute solid and liquid solutions in coexistence.

There are vast numbers of problems both in the chemical industry and in the natural world that depend on the partitioning of chemical components between coexisting phases, and the ability to calculate chemical potentials *ab initio* should make it possible to address some of these problems in a new way. Our original incentive for developing these techniques was the desire to understand better the chemistry of the Earth's core, and this is a good example of a problem where *ab initio* calculations can supply information that is difficult to obtain experimentally because of the extreme conditions of temperature ($T \sim 6000$ K) and pressure ($p \sim 330$ GPa). The core is composed mainly of Fe, and comprises an outer liquid part and an inner solid part [24]. The density of the outer core is ~ 6 % too low to be pure Fe [24, 25, 26, 27, 28], and cosmochemical and geochemical arguments show that the main light impurities are probably S, O and Si [26]. The inner core has grown over geological time by crystallisation from the outer core, and the partitioning of impurities between liquid and solid is crucial for understanding the evolution and contemporary dynamics of the core. The size of the density discontinuity (*ca.* 4.5 %) [29, 30] at the inner-core/outer-core boundary can only be interpreted if one understands this partitioning, and also provides a constraint on possible chemical compositions. We shall show how our *ab initio* techniques for calculating chemical potentials shed completely new light on this problem. Brief reports of these calculations have already appeared [27, 31, 32].

In developing the theoretical basis of our techniques, we define our technical aims in Sec. 2 by summarising the standard thermodynamic relations describing phase equilibrium. The difference of chemical potentials of solute and solvent atoms, and the free energy change associated with the transmutation of solvent into solute are discussed in Sec. 3. In Sec. 4, we then develop the *ab initio* techniques themselves. We shall explain how thermodynamic integration can be used to perform the solvent-solute transmutation so as to obtain the difference of chemical

potentials in the liquid; we also describe the techniques for calculating chemical potentials in solid solutions, both in the harmonic approximation and using thermodynamic integration to handle anharmonicity. Sec. 5 presents our results for the case of S, O and Si dissolved in solid and liquid Fe under Earth's core conditions, and summarizes the implications of the results for the partitioning of these impurities between the inner and outer core and the chemical composition of the core. Discussion and conclusions are given in Sec. 6.

2   Chemical equilibrium: thermodynamics

Our task in this Section is to identify the thermodynamic quantities that will need to be calculated *ab initio*. Chemical equilibrium between two multicomponent phases is characterized by equality of the chemical potentials of each component in the two phases. For a two-component solution consisting of solute X dissolved in solvent A, equilibrium between solid and liquid phases requires that:

$$\mu_X^l(p, T_m, c_X^l) = \mu_X^s(p, T_m, c_X^s) \, , \tag{1}$$

$$\mu_A^l(p, T_m, c_X^l) = \mu_A^s(p, T_m, c_X^s) \, , \tag{2}$$

where μ_X and μ_A are the chemical potentials of solute and solvent, p is the pressure and c_X is the mole fraction of solute, with superscripts l and s for liquid and solid respectively; T_m is the melting temperature, i.e. the temperature at which the liquid and solid solutions are in equilibrium, which depends on the impurity mole fractions. The two equations impose two relations between c_X^l, c_X^s and T_m at the given p. In the low-concentration limit $c_X \to 0$, μ_X diverges logarithmically, and it is useful to write:

$$\mu_X(p, T, c_X) = k_B T \ln c_X + \tilde{\mu}_X(p, T, c_X) \, , \tag{3}$$

where $\tilde{\mu}_X(p, T, c_X)$ is well behaved for all c_X. In an ideal solution, $\tilde{\mu}_X$ is independent of c_X, but in reality the interaction between solute atoms causes it to vary with c_X. Combining Eqs. (1) (3), we obtain:

$$c_X^s / c_X^l = \exp[(\tilde{\mu}_X^l - \tilde{\mu}_X^s)/k_B T_m] \, , \tag{4}$$

so that the ratio of the mole fractions c_X^s and c_X^l in solid and liquid is determined by the thermodynamic quantities $\tilde{\mu}_X^l$ and $\tilde{\mu}_X^s$. The melting temperature T_m entering Eq. (4) differs from the melting temperature T_m^0 of the pure solvent, and may be regarded as determined by Eq. (2).

We now develop a practical way of solving Eqs. (2) and (4). We are interested in the case of moderately low c_X, but we wish to take account of the variation of $\tilde{\mu}_X$ with c_X to lowest order. We therefore expand $\tilde{\mu}_X$ as:

$$\tilde{\mu}_X(p, T, c_X) = \mu_X^\dagger(p, T) + \lambda_X(p, T)c_X + O(c_X^2) \, , \tag{5}$$

and we shall systematically neglect the terms $O(c_X^2)$. Since it will be important later, we stress here that this represents the concentration dependence of $\tilde{\mu}_X$ at constant pressure. Eq. (4) then becomes:

$$c_X^s / c_X^l = \exp\left[(\mu_X^{\dagger l} - \mu_X^{\dagger s} + \lambda_X^l c_X^l - \lambda_X^s c_X^s)/k_B T_m\right] \, . \tag{6}$$

To obtain an equation for T_m, we need the corresponding expansion for μ_A. We use the Gibbs-Duhem equation:

$$c_A d\mu_A + c_X d\mu_X = 0 \, , \tag{7}$$

which gives:

$$\mu_A(p, T, c_X) = \mu_A^0(p, T) + (k_B T + \lambda_X(p, T)) \ln(1 - c_X) + \lambda_X(p, T)c_X + O(c_X^2) \, , \tag{8}$$

where μ_A^0 is the chemical potential of the pure solvent, and we have used the fact that $c_A = 1 - c_X$. To linear order in c_X, this gives:

$$\mu_A(p, T, c_X) = \mu_A^0(p, T) - k_B T c_X + O(c_X^2) . \tag{9}$$

We apply this in Eq. (2) by expanding $\mu_A^0(p, T)$ to linear order in the difference $T_m - T_m^0$ between T_m and the melting temperature T_m^0 of pure solvent. This yields:

$$- k_B T_m c_X^l + \mu_A^{0l}(p, T_m^0) + (T_m - T_m^0) \left(\frac{\partial \mu_A^{0l}}{\partial T} \right)_{T=T_m^0} =$$
$$- k_B T_m c_X^s + \mu_A^{0s}(p, T_m^0) \quad + \quad (T_m - T_m^0) \left(\frac{\partial \mu_A^{0s}}{\partial T} \right)_{T=T_m^0} . \tag{10}$$

Since $\mu_A^{0s}(p, T_m^0) = \mu_A^{0s}(p, T_m^0)$, we can rewrite this equation as:

$$k_B T_m c_X^l + (T_m - T_m^0) s_A^{0l} = k_B T_m c_X^s + (T_m - T_m^0) s_A^{0s}, \tag{11}$$

where $s_A^0 = - (\partial \mu_A^0 / \partial T)_{T=T_m^0}$ is the entropy per atom of pure solvent at the melting temperature. The shift of melting temperature due to the presence of the solute is then:

$$(T_m - T_m^0) = \frac{k_B T_m}{\Delta s_A^0} (c_X^s - c_X^l) , \tag{12}$$

where $\Delta s_A^0 \equiv s_A^{0l} - s_A^{0s}$ is the entropy of fusion of pure solvent. Eqs. (6) and (12) must be solved self-consistently.

We see from Eqs. (6) and (12) that the main thermodynamic quantities to be calculated *ab initio* are $\mu_X^\dagger$ and λ_X for the solid and liquid solution. We also require *ab initio* values for the melting temperature and entropy of fusion of pure solvent. In addition, we shall find it necessary to obtain *ab initio* values of the partial molar volumes of the solute, which will be discussed later. We next turn to the statistical-mechanical considerations needed to develop a strategy for calculating $\mu_X^\dagger$ and λ_X.

3   Interconversion of solvent and solute: statistical mechanics

The chemical potential of a solute X in solid or liquid solvent A is the change of Gibbs free energy when one atom of X is added to the system at constant pressure and temperature. In our practical *ab initio* calculations, we work at constant volume rather than constant pressure, so we prefer the equivalent statement that the solute chemical potential is the change of Helmholtz free energy when the solute atom is added at constant volume and temperature. However, it is impractical to add solute atoms to a system in an *ab-initio* simulation. It is more convenient to convert solvent into solute, which means working with the difference $\mu_X - \mu_A$ of the chemical potentials. The chemical potential μ_X and hence $\tilde{\mu}_X$ can then be obtained from $\mu_X - \mu_A$ by making use of the Gibbs free energies of pure solid and liquid A, calculated separately. We have sketched this technique briefly in our previous papers [27, 31, 32], and we now describe it in more detail.

The Helmholtz free energy of a system containing N_A solvent atoms and N_X solute atoms is:

$$F(N_A, N_X) = -k_B T \ln \left\{ \frac{1}{N_A! N_X! \Lambda_A^{3N_A} \Lambda_X^{3N_X}} \int_V d\mathbf{R} \exp \left[-\beta U(N_A, N_X; \mathbf{R}) \right] \right\} , \tag{13}$$

where $\beta = 1/k_B T$, and Λ_X and Λ_X are the thermal wavelengths of A and X, given by $\Lambda_A = h/(2\pi M_A k_B T)^{1/2}$, with M_A the atomic mass of A, and similarly for Λ_X. The quantity $U(N_A, N_X; \mathbf{R})$ is the total energy function of the system of N_A solvent and N_X solute

atoms, which depends on the positions of all the atoms, indicated by $\mathbf{R}$, and $\int_V d\mathbf{R}$ indicates integration over the whole configuration space of the system contained in volume V.

The difference of chemical potentials $\mu_{XA} \equiv \mu_X - \mu_A$ is equal to the change of F when a single atom of A is converted into X, and is given by:

$$
\begin{aligned}
\mu_{XA} &= F(N_A - 1, N_X + 1) - F(N_A, N_X) \\
&= -k_B T \ln(N_A/N_X) - k_B T \ln\left(\Lambda_A^3/\Lambda_X^3\right) \\
&\quad - k_B T \ln\left\{ \frac{\int_V d\mathbf{R} \exp\left[-\beta U(N_A - 1, N_X + 1; \mathbf{R})\right]}{\int_V d\mathbf{R} \exp\left[-\beta U(N_A, N_X; \mathbf{R})\right]} \right\} .
\end{aligned}
\tag{14}
$$

We express this as:

$$
\mu_{XA} = k_B T \ln \frac{c_X}{1 - c_X} + 3k_B T \ln \frac{\Lambda_X}{\Lambda_A} + m(c_X) ,
\tag{15}
$$

where we define:

$$
m(c_X) = -k_B T \ln\left\{ \frac{\int_V d\mathbf{R} \exp\left[-\beta U(N_A - 1, N_X + 1; \mathbf{R})\right]}{\int_V d\mathbf{R} \exp\left[-\beta U(N_A, N_X; \mathbf{R})\right]} \right\} .
\tag{16}
$$

The intensive quantity $m(c_X)$ depends only on pressure, temperature and concentration (we write it as $m(p, T, c_X)$), or alternatively on volume, temperature and concentration (we then write it as $m(\bar{v}, T, c_X)$, where $\bar{v}$ is the mean atomic volume $V/(N_A + N_X)$). Expanding Eq. (15) to linear order in c_X, we have:

$$
\mu_{XA} = k_B T \ln c_X + k_B T c_X + 3k_B T \ln \frac{\Lambda_X}{\Lambda_A} + m(c_X).
\tag{17}
$$

Compare now with Eqs. (3), (5) and (9):

$$
\mu_{XA} = k_B T \ln c_X + \mu_X^\dagger + \lambda_X c_X - \mu_A^0 + k_B T c_X ,
\tag{18}
$$

and we have:

$$
m(c_X) + 3k_B T \ln \frac{\Lambda_X}{\Lambda_A} = \mu_X^\dagger - \mu_A^0 + \lambda_X c_X.
\tag{19}
$$

If values are available for $m(p, T, c_X)$ at different values of c_X for a given pressure p, we can obtain the quantities $\mu_{XA}^\dagger \equiv \mu_X^\dagger - \mu_A^0 - 3k_B T \ln(\Lambda_X/\Lambda_A)$ and λ_X for that pressure. We then need the pure-solvent chemical potentials μ_A^0 for liquid and solid, whose *ab initio* calculation has been described in detail elsewhere [9, 17, 18].

We conclude this Section by rewriting c_X^s/c_X^l from Eq. (4) in terms of $\mu_{XA}^\dagger$, λ_X and μ_A^0 for liquid and solid:

$$
c_X^s/c_X^l = \frac{\exp\left[\left(\mu_{XA}^{\dagger l} - \mu_{XA}^{\dagger s} + \lambda_X^l c_X^l - \lambda_X^s c_X^s\right)/k_B T_m\right]}{\exp\left[\left(\mu_A^{0s} - \mu_A^{0l}\right)/k_B T_m\right]} .
\tag{20}
$$

If the concentrations are small enough for the difference between T_m and T_m^0 to be negligible, then $\mu_A^{0s} = \mu_A^{0l}$, and the denominator is unity; but in general deviations of the denominator from unity should be included.

4 Ab initio chemical potentials

4.1 The liquid solution

For the liquid, we calculate the quantity $m(c_X)$ of Eq. (16) by a form of 'thermodynamic integration'. We first outline a simple way of doing this that is correct in principle, but suffers

from practical problems; we then show how the method can be modified to give a practical procedure.

Thermodynamic integration [33] is a general technique for computing the Helmholtz free energy difference $F_1 - F_0$ of two systems containing the same number N of atoms, but having different total energy functions $U_1(\mathbf{R})$ and $U_0(\mathbf{R})$. The difference $F_1 - F_0$ is the reversible work done on continuously switching the total energy function from U_0 to U_1 at constant volume, which is given by

$$F_1 - F_0 = \int_0^1 d\lambda \, \langle U_1 - U_0 \rangle_\lambda \,, \tag{21}$$

where the average $\langle \cdot \rangle$ is calculated in thermal equilibrium for the system governed by the 'hybrid' energy function $U_\lambda \equiv (1 - \lambda)U_0 + \lambda U_1$. This is a well established technique for the *ab initio* calculation of liquid-state free energies [15, 16], which was used in our recent *ab initio* investigation [9, 17, 18] of the high pressure melting curve of Fe.

In order to compute $m(c_X)$, we could in principle choose U_0 to be the total energy for the system of N_A atoms of solvent and N_X of solute, and U_1 to be the same for $N_A - 1$ atoms of A and $N_X + 1$ of X. We evaluate $\langle U_1 - U_0 \rangle_\lambda$ by performing *ab initio* molecular dynamics with time evolution generated by U_λ, and taking the time average of $U_1 - U_0$. This is repeated for several values of λ, and the integration over λ is done numerically. This type of 'alchemical' transmutation of A into X obviously does not correspond to a real-world process, but in terms of *ab initio* statistical mechanics is a perfectly rigorous way of obtaining the quantity $m(c_X)$. It demands an unusual kind of simulation: For the atom positions $\mathbf{r}_1, \ldots \mathbf{r}_N$ at each instant of time, we have to perform two independent *ab initio* calculations, one for each chemical composition. As well as U_0 and U_1 for the given positions, we calculate two sets of *ab initio* forces $\mathbf{F}_{0i} \equiv -\nabla_i U_0$ and $\mathbf{F}_{1i} \equiv -\nabla_i U_1$, and the linear combinations $\mathbf{F}_{\lambda i} \equiv (1 - \lambda)\mathbf{F}_{0i} + \lambda \mathbf{F}_{1i}$ are used to generate the time evolution.

The major problem with this scheme is one of statistics. The thermal average $\langle \cdot \rangle_\lambda$ is evaluated as a time average, but since only a single atom is transmuted the scheme does not benefit from averaging over atoms. The efficiency of the averaging can be considerably improved if one is prepared to transmute several atoms simultaneously. If we do this, then instead of obtaining $m(c_X)$ at a given mole fraction c_X, we obtain an integral of $m(c_X)$ over a range of c_X values. The information we need can still be extracted, as we now describe.

Consider the change of Helmholtz free energy when we start from N atoms of pure solvent and transmute N_X of them into solute atoms at constant volume and temperature. This can clearly be calculated by thermodynamic integration using the procedure outlined above. Denoting this change of free energy by $W(N, N_X)$, we can express it as:

$$W(N, N_X) = -k_B T \ln \left\{ \frac{\int_V d\mathbf{R} \exp\left[-\beta U(N - N_X, N_X; \mathbf{R})\right]}{\int_V d\mathbf{R} \exp\left[-\beta U(N, 0; \mathbf{R})\right]} \right\} . \tag{22}$$

We then have:

$$W(N, N_X) = \int_0^1 d\lambda \, \langle U_1 - U_0 \rangle_\lambda \,, \tag{23}$$

with $U_1(\mathbf{R}) = U(N - N_X, N_X; \mathbf{R})$ and $U_0(\mathbf{R}) = U(N, 0; \mathbf{R})$. Our procedure will be to calculate $W(N, N_X)$ at several values of $N_X/N = c_X$ at a chosen volume, and then fit the results in the following way:

$$W(N, N_X)/N_X = a + bc_X . \tag{24}$$

The information needed can now be extracted by noting that for a given mean atomic volume $\bar{v}$, the quantity $m(\bar{v}, T, c_X)$ is:

$$m(\bar{v}, T, c_X) = (\partial W/\partial N_X)_{V,T} = a + 2bc_X . \tag{25}$$

It follows immediately that:

$$\mu_{XA}^\dagger = \lim_{c_X \to 0} m(\bar{v}, T, c_X) = a . \tag{26}$$

To obtain λ_X from the coefficient b, we note that $\lambda_X = \lim_{c_X \to 0}(\partial m(p, T, c_X)/\partial c_X)_p$ and $2b = \lim_{c_X \to 0}(\partial m(\bar{v}, T, c_X/\partial c_X)_{\bar{v}}$. The fact that one derivative is isobaric and the other isochoric is significant. The quantity λ_X that we seek describes the isobaric concentration dependence of solute chemical potential. But since our *ab initio* calculations are done at fixed volume, the immediately available quantity b is an isochoric derivative.

The relation between the constant-pressure and constant-volume derivatives of m is examined in the Appendix, where we show that:

$$(\partial m/\partial c_X)_p = (\partial m/\partial c_X)_{\bar{v}} - nB_T(v_X - v_A)^2 , \qquad (27)$$

where B_T is the isothermal bulk modulus, and v_X and v_A are the partial atomic volumes of solute and solvent. We conclude that:

$$\lambda_X = 2b - nB_T(v_X - v_A)^2 . \qquad (28)$$

Here, the quantities B_T, v_X and v_A can be evaluated at infinite dilution. The calculation of B_T and v_A involves only *ab initio* m.d. simulations on the pure solvent, and presents no problem. We return below (Sec. 4.3) to the *ab initio* calculation of v_X. With this, we have a complete procedure for determining $\mu_{XA}^{\dagger}$ and λ_X.

4.2 The solid solution

If anharmonic effects are negligible, then the free energy of the solid can be obtained from *ab initio* phonon frequencies, so that thermodynamic integration is not needed, and no statistical averaging is involved in the *ab initio* calculations. There is then nothing to prevent us from calculating $m(c_X)$ directly from the free energy change when solvent atoms are replaced by solute atoms. We assume for the moment that this is adequate, and return later to the question of anharmonic effects.

We start by considering the zero-concentration limit of $m(c_X)$, namely $\mu_{XA}^{\dagger}$, which is the non-configurational free energy change when an atom in the perfect A crystal is replaced by an X atom. This can be written as:

$$\mu_{XA}^{\dagger} = \mu_{XA}^{\dagger \, \mathrm{perf}} + \mu_{XA}^{\dagger \, \mathrm{harm}} , \qquad (29)$$

where $\mu_{XA}^{\dagger \, \mathrm{perf}}$ is the free energy change for the perfect non-vibrating crystal, and $\mu_{XA}^{\dagger \, \mathrm{harm}}$ is the harmonic vibrational part – we refer to $\mu_{XA}^{\dagger \, \mathrm{perf}}$ as a 'free energy' to allow for the possibility of thermal electronic excitations, which are important in high-temperature Fe [9]. The calculation of $\mu_{XA}^{\dagger \, \mathrm{perf}}$ is straightforward, and involves only the difference of *ab initio* (free) energies of the static fully relaxed crystal containing a single substitutional X atom and the static perfect crystal, the two systems having the same volume.

In the high-temperature limit, where T is well above the Debye temperature, $\mu_{XA}^{\dagger \, \mathrm{harm}}$ can be written as:

$$\mu_{XA}^{\dagger \, \mathrm{harm}} = k_B T \sum_n \ln \left(\omega_n'/\omega_n \right) , \qquad (30)$$

where ω_n' and ω_n are the harmonic frequencies of the normal modes of the impure and pure crystals, and the sum goes over all modes. The frequencies are calculated *ab initio*, and we use the 'small-displacement' method described in detail elsewhere [9, 34, 35]. This involves DFT calculations of the force on every atom in the system induced by displacement of a single atom, and this has to be done for all symmetry inequivalent atoms and displacements. To obtain λ_X in the harmonic approximation, we must include the effect of interactions between solute atoms. The key to this is to note that the calculation of the partition function, i.e. the integral over configuration space of Eq. (13), can be broken into (a) a sum of distinct configurations, i.e. assignments of solute atoms to lattice sites, and (b) an integral over vibrational displacements

of the atoms away from their relaxed equilibrium positions for each such configuration. This means that the statistical mechanics of the solid solution maps exactly onto that of a lattice gas, and the free energy of the solid solution is:

$$F(N_A, N_X) = -k_B T \ln \left(\sum_\gamma e^{-\beta \Phi_\gamma} \right) , \tag{31}$$

where the sum goes over all distinct configurations γ, and Φ_γ is the non-configurational free energy of the system for each γ.

It is convenient to relate $F(N_A, N_X)$ to the free energy F_A of the pure A crystal having the same number of lattice sites. The difference $\Delta F(N, N_X) \equiv F(N_A, N_X) - F_A$ is the change of free energy when N_X atoms of A in the pure crystal are transmuted into X atoms. We have:

$$\Delta F(N_A, N_X) = -k_B T \ln \left(\sum_\gamma e^{-\beta(\Phi_\gamma - F_A)} \right) . \tag{32}$$

Now in the limit $c_X \to 0$, we can neglect the interactions between X atoms, and we get:

$$\Phi_\gamma - F_A \to N_X \mu_{XA}^\dagger . \tag{33}$$

At higher concentrations, we need to include the free energy of interaction between pairs of X atoms, and we write:

$$\Phi_\gamma - F_A \simeq N_X \mu_{XA}^\dagger + \frac{1}{2} \sum_{m \neq n} \phi_{mn} , \tag{34}$$

where ϕ_{mn} is the non-configurational free energy change when a pair of X atoms are brought from widely separated sites in the otherwise perfect crystal to the sites m and n. We then have:

$$\Delta F(N, N_X) = N_X \mu_{XA}^\dagger - k_B T \ln \left(\sum_\gamma \exp \left[-\frac{1}{2} \beta \sum_{m \neq n} \phi_{mn} \right] \right) . \tag{35}$$

In the later practical calculations, we approximate by setting ϕ_{mn} equal to zero except when m and n are nearest-neighbor lattice sites, the interaction free energy being then called simply ϕ.

It is now an exercise in the statistical mechanics of lattice gases to show that the leading order in c_X:

$$\Delta F(N, N_X) = N_X \mu_{XA}^\dagger \quad + \quad N k_B T \left[c_X \ln c_X + (1 - c_X) \ln c_X \right] +$$
$$+ \quad \frac{1}{2} N k_B T c_X^2 z \left(1 - e^{-\beta\phi} \right) , \tag{36}$$

where z is the coordination number of the lattice. The derivative $\partial \Delta F(N, N_X)/\partial N_X$ gives us $\mu_X - \mu_A$, from which we straightforwardly extract λ_X, which is given by:

$$\lambda_X = k_B T z \left(1 - e^{-\beta\phi} \right) . \tag{37}$$

As in the case of the liquid, this formula should be corrected from constant volume to constant pressure, so that the correct formula is:

$$\lambda_X = k_B T z \left(1 - e^{-\beta\phi} \right) - n B_T (v_X - v_A)^2 , \tag{38}$$

with B_T, v_X and v_A the isothermal bulk modulus and partial molar volumes in the dilute solid solution. The calculation of B_T and v_A presents no problems; we return to the *ab initio* calculation of v_X in Sec. 4.3.

In addition to using this analytic derivation to obtain λ_X, we have also performed Monte Carlo calculations on the lattice gas to obtain numerical values of $\Delta F(N, N_X)$. These serve

both to confirm the correctness of the analytic result in the region of low c_X and also to assess deviations from the linear dependence of $\tilde{\mu}_X$ on c_X as c_X increases.

The remaining task is to calculate the nearest-neighbor interaction free energy ϕ. This follows exactly the scheme for calculating $\mu^\dagger_{XA}$, where now ϕ is the non-configurational free-energy change when two neighboring atoms in the perfect crystal A are replaced by X atoms, minus twice $\mu^\dagger_{XA}$. This can be written as:

$$\phi = \phi^{\mathrm{perf}} + \phi^{\mathrm{harm}} \,, \tag{39}$$

where ϕ^{perf} is the (free) energy change for the perfect non-vibrating crystal, and ϕ^{harm} is the harmonic vibrational part. The static part ϕ^{perf} is obtained from the difference of *ab initio* free energies of the relaxed equilibrium system containing neighboring X atoms and the perfect pure A lattice. We obtain ϕ^{harm} from the harmonic vibrational frequencies of the system containing the neighboring X atoms by a formula exactly analogous to Eq. (30).

We now return very briefly to the question of anharmonicity. In many cases, very high precision may not be needed for the chemical potentials, so that anharmonic corrections to $\tilde{\mu}^s_X$ can be neglected. But in one case that will be important later, that of substitutional O in Fe, we know that anharmonic effects are large. The techniques we have used to treat them are described in detail elsewhere [31]. The strategy is based on thermodynamic integration between reference models representing both the pure Fe and the impure Fe/X systems, followed by further thermodynamic integrations between the *ab initio* and reference systems.

4.3 Partial molar volumes in the liquid and solid solutions

The partial molar volume v_X of solute or v_A of solvent is the change of volume of the system when one atom of X or A is added at constant pressure and temperature. The volumes are related to the chemical potentials by:

$$v_X = (\partial \mu_X / \partial p)_{T,c_X} \,, \qquad v_A = (\partial \mu_A / \partial p)_{T,c_X} \,. \tag{40}$$

We note that the total volume of the system is given by $V = N_X v_X + N_A v_A$. As for the chemical potentials, we find it easier to consider the interconversion of solvent and solute, and to work with the difference $v_{XA} \equiv v_X - v_A$. The liquid is treated by *ab initio* m.d., in which the pressure for a given volume is calculated during the simulation. (In our practical calculations, we work at constant V.) The straightforward way of obtaining the dilute limit of v_X is therefore to calculate the change of pressure Δp resulting from the replacement of a chosen number N_X of atoms in the pure solvent by X. The pressure change per atom $\delta p = \Delta p / N_X$ then gives us v_{XA} by the relation $v_{XA} = V \delta p / B_T$.

It is clearly possible to follow the same route for the solid. However, if the solid is treated by harmonic frequency calculations with or without thermodynamic integration for the anharmonic contribution, then the partial molar volumes must be obtained from the chemical potentials *via* Eq. (40). This requires calculation of μ_X at different volumes followed by numerical differentiation.

5 Illustration: chemical equilibrium in the Earth's core

In applying the techniques to study chemical phase equilibrium between the Earth's inner and outer core, our aim is to show how they can yield important new information about the chemical composition and temperature of the core, both of which are controversial. Our strategy exploits the fact that that the density as a function of depth in the core is accurately known from seismic measurements [30]; in particular, it is quite well established that there is a density discontinuity of 4.5 ± 0.5 % across the inner-core/outer-core boundary (ICB) [29]. Recent *ab initio* studies of the melting properties of pure Fe concur in giving a volume of

fusion of ~ 1.8 % [18, 28], which is clearly much smaller. This means that there must be a substantial partitioning of light solute elements from solid to liquid to account for the large observed discontinuity.

This discontinuity can be studied with our methods. If we suppose initially that the core is a binary solution of Fe with one of the leading impurity condidates S, Si or O [26], then the solute mole fraction in the liquid core can be fixed by requiring that the density reproduce the seismically observed density. Calculation of the chemical potentials μ_X in the liquid and solid then gives us the mole fraction in the solid, from which we can deduce the solid density, and hence the density discontinuity. Agreement or disagreement with the known discontinuity puts a constraint on the composition. At the same time, the shift of melting temperature given by Eq. (12) gives us information about the temperature at the ICB.

In the following, we first summarize the general techniques used in all the calculations (Sec. 5.1). We then describe separately the calculations on the liquid and solid alloys (Sec. 5.2 and 5.3 respectively), presenting results for the chemical potentials and partial molar volumes. In Sec. 5.4, we then combine the results with seismic data to obtain constraints on the chemical composition and temperature of the Earth's core.

5.1   General techniques

Our *ab initio* calculations are based on the well established DFT methods used in virtually all *ab initio* investigations of solid and liquid Fe [9, 17, 18, 36, 37, 38, 39], including our own previous work on pure Fe and its solid and liquid alloys with S and O [27, 31, 40, 41]. We employ the generalized gradient approximation for exchange-correlation energy, as formulated by Perdew *et al.* [42], which is known to give very accurate results for the low-pressure elastic, vibrational and magnetic properties of body-centred cubic (b.c.c.) Fe, the b.c.c. $\rightarrow$ h.c.p. transition pressure, and the pressure-volume relation for h.c.p. Fe up to over 300 GPa [36, 39]. There is also very recent evidence for their accuracy in predicting the high-pressure phonon spectrum of h.c.p. Fe [43]. We use the ultra-soft pseudopotential implementation [44] of DFT with plane-wave basis sets, an approach which has been demonstrated to give results for solid Fe that are virtually identical to those of all-electron DFT methods [39]. Our calculations are performed using the VASP code [45], which is exceptionally stable and efficient for metals. We implemented a scheme for the extrapolation of the charge density which increases the efficiency of the molecular dynamics simulations by nearly a factor of two [46]. The technical details of pseudopotentials, plane-wave cut-offs, etc. are the same as in our previous work [41].

5.2   The liquid

Our *ab initio* m.d. simulations on the liquid, which we used to calculate $W(N, N_X)$ and hence the chemical potentials, were all performed on systems of 64 atoms, with a time-step of 1 fs and with Γ-point sampling of the electronic Brillouin zone. In our previous calculations on pure liquid Fe [18], we showed that Γ-point sampling on a 67-atom cell underestimates the free energy by *ca.* 10 meV/atom; this is a completely negligible error for present purposes. The calculations were done at $T = 7000$ K and at the volume/atom $V/N = 6.97$ Å/atom, which for pure Fe gives a pressure of 370 GPa. This pressure is somewhat higher than the ICB pressure of 330 GPa [30]. The temperature is also higher than that at the ICB: our *ab initio* melting curve gives a melting temperature of ~ 6350 K (or ~ 6200 K after the correction due to our estimate of likely DFT errors) [18] at the ICB pressure of 330 GPa, which is already higher than some other estimates [28, 47]. But we shall see below that depression of freezing point due to impurity partitioning lowers this by a further ~ 700 K. We have made rough estimates which show that the difference between 7000 K and our estimated ICB temperature is unlikely to change the chemical potentials of S and Si by more than 0.1 eV and that of O by more than 0.3 eV, which will have no significant effect on our conclusions. The difference of pressures should also make little difference.

We have used thermodynamic integration to calculate $W(N, N_X)$ for the three solute elements S, Si and O for $N_X = 3$, 6 and 12, corresponding to mole fractions of 4.7, 9.4 and 18.8 %. In doing this, we have aimed to choose the number of λ values large enough and the duration of the simulation at each λ value long enough to give a precision on $W(N, N_X)/N_X$ of *ca.* 0.05 eV for S and Si and *ca.* 0.1 eV for O. To illustrate how the thermal average $\langle U_1 - U_0 \rangle_\lambda$ in Eq. (23) depends on λ, we display this quantity in Fig. 1 at five equally spaced λ values for the oxygen system with $N_X = 12$. We see that the dependence on λ is not far from linear. Using Simpson's rule to perform the integral, we compared results for $W(N, N_X)/N_X$ using the five λ values 0.0, 0.25, 0.50, 0.75 and 1.00 with those obtained using only the three values 0.0, 0.5 and 1.0, and found that they differ by less than the statistical error. Since the replacement of Fe by O is a greater perturbation than that of Fe by S or Si (see below), we have taken this as justification for using only three λ values in all the thermodynamic integrations. Our numerical results for $W(N, N_X)/N_X$ for X = S, Si and O, together with the linear least-square fit of Eq. (24), are reported in Fig. 2, and the resulting values of $a \equiv \mu_{XA}^\dagger$ and b are given in Table 1.

As explained in Sec. 4.1, the b values have to be corrected as in Eq. (28) in order to obtain λ_X, and this requires the partial molar volumes v_X. We obtain the partial molar volumes from the simulations just described by studying the pressure change resulting from the replacement of N_X atoms in the pure liquid by atoms of X at constant volume – this is straightforward, since the pressure is automatically calculated during the constant-volume simulations. We find that within the statistical errors the change of pressure is linear in c_X for all three impurity species. We then use the fact that $v_X - v_A = (\bar{v}/B_T)(\partial p/\partial c_X)_T$; for B_T we use the bulk modulus of the pure liquid, which we know from our previous work [18]. The calculated v_X values are 6.65, 6.65 and 4.25 Å^3 for S, Si and O respectively, compared with the volume per atom in the pure liquid of 6.97 Å^3. We note that S and Si have almost exactly the same volume as Fe, but that the volume of O is considerably smaller. Using these v_X values in Eq. (28), we now obtain the results for λ_X given in Table 1. We see that the difference between $2b$ and λ_X is very small for sulfur and silicon, as expected, but is substantial for oxygen.

5.3 The solid

The available evidence strongly indicates that the stable crystal structure of Fe at the pressures and temperatures of the Earth's core is hexagonal close packed (h.c.p.) [48], and this is the structure adopted in our calculations. We first present our calculations for S and Si, and then summarize briefly our results for the more complex case of O, which have already been reported elsewhere.

5.3.1 Sulfur and silicon

The calculations are performed on a $4\times4\times2$ h.c.p. supercell containing 64 atoms, with a $3\times3\times2$ Monkhorst-Pack [49] grid of electronic k-points which give free energies converged within a few meV/atom. In our calculations on the static zero-temperature lattice, we find that when a single Fe is replaced by S or Si at constant volume, the relaxation of neighboring atoms is very small, and the pressure change is also small. For the atomic volume $v = 6.97$ Å^3/atom, the partial molar volumes calculated without lattice vibrations give the differences $v_S - v_{Fe} = -0.32$ and $v_{Si} - v_{Fe} = -0.32$ Å^3, which are extremely small compared with v_{Fe}. We assume that that these differences will not be significantly affected by thermal effects.

We now turn to the harmonic frequencies ω_n and ω_n' needed for the harmonic difference of chemical potentials $\mu_{XA}^{\dagger\text{harm}}$ (see Eq. (30)). We calculate these using a supercell of 64 atoms in all calculations. For the pure Fe system only two independent displacements of a single atom are needed to obtain the full force constant matrix [9]. We displace the atom by *ca.* 0.015 Å in each direction, which is known to be small enough to ensure accurate linearity between forces and displacements. For the calculations where one Fe is substituted with S or Si, the symmetry

is much reduced, and the number of atoms to be displaced is 15, with the total number of independent displacements being 33. For the systems with two solute atoms, the symmetry of the system is reduced even further, and we need to displace 20 atoms in all possible directions, for a total of 60 displacements. There are two distinct ways of putting two S or Si atoms on nearest-neighbor sites: the first has both sites in the same basal plane, and the second has them in adjacent basal places. Within our errors, we cannot detect the free energy difference between the two arrangements. Since the zero temperature value of the difference $v_X - v_{Fe}$ is very small, we have not attempted to calculate its high temperature value in the harmonic approximation, and we report in Table 1 the zero temperature value. The correction to λ_X is negligible anyway and can be ignored.

For sulfur and silicon we neglect anharmonic corrections. In our previous work on pure Fe [9] we showed that at ICB conditions the anharmonic contribution to the free energy is roughly 60 meV/atom. In this case we are concerned with free energy differences between the pure Fe system and a system where one of the Fe atoms has been substituted with X, so the difference of the relative anharmonic contributions to the free energies is presumably smaller than that.

Our calculated values of $\mu_{XA}^{\dagger s}$ and λ_X^s at $v = 6.97$ Å^3/atom and $T = 7000$ K are reported in Table 1.

5.3.2 Oxygen

As emphasized above and in previous work [31], substitutional O in h.c.p. Fe is highly anharmonic, because O is considerably smaller than Fe and has great freedom of movement, so that the harmonic approximation is completely inadequate for calculating $\mu_{O\,Fe}^{\dagger s}$. We gave a brief summary in Sec. 4.2 of the thermodynamic integration techniques used to do the calculations. The numerical result for $\mu_{O\,Fe}^{\dagger s}$ at $v = 6.97$ Å^3/atom and $T = 7000$ K is reported in Table 1. We have not attempted to calculate λ_X for X = O, since this would be extremely demanding, and turns out to be unnecessary in our analysis of core composition.

To calculate $v_O - v_{Fe}$ in the solid we have repeated the calculations at different volumes and numerically differentiated the results, as described in section 4.3. The value of $v_O - v_{Fe}$ is reported in Table 1.

5.4 Core composition and temperature

Some crucial features of our results are immediately clear from Table 1: the liquid-solid difference $\mu_{XA}^{\dagger l} - \mu_{XA}^{\dagger s}$ is negative in all cases; its magnitude is somewhat smaller than $k_B T$ for S and Si, but is much bigger than $k_B T$ for O. This implies that the solutes will all partition from solid into liquid, as expected; but the partitioning will be weak for S and Si and very strong for O.

To see the implications in more detail, consider the case of Fe/S. If we postulate that the core is an Fe/S binary alloy, then we can estimate the mole fraction c_S^l in the outer core by noting that the density of pure liquid iron at the ICB pressure is $ca.$ 6 % higher than the values obtained from seismic data [30]. We therefore add sulfur to the liquid until the density is reduced to the required value, which gives $c_S^l = 0.16$. Now if we ignored the dependence of $\tilde{\mu}_S$ on concentration, then the value $\mu_S^{\dagger l} - \mu_S^{\dagger s} = -0.25$ eV would give $c_S^s/c_S^l = 0.66$, so that $c_S^s = 0.11$. However, the positive λ_S values mean that both $\tilde{\mu}_S^l$ and $\tilde{\mu}_S^s$ increase strongly with increasing mole fraction of S, and this will tend to equalize the mole fractions in solid and liquid. If we solve Eq. (4) self-consistently for c_S^s with the given c_S^l, we find $c_S^s = 0.14$. But a 14 % mole fraction of S in the inner core is completely incompatible with the seismic measurements. We can use the c_S^s volume together with the partial molar volume v_S^s to calculate the change of density of the solid due to dissolved S, and hence the ICB density discontinuity. We find the discontinuity is increased from the pure-Fe value of 1.8 % up to 2.7 ± 0.5 %, which is still

much less than the seismic value of 4.5 ± 0.5 %. This means that the binary Fe/S alloy can be ruled out as a model for core composition. The argument is still stronger for Si, since the chemical potentials in solid and liquid are even more similar than for S. We conclude that the binary Fe/Si model must also be ruled out.

For O, the situation is the opposite. The difference of chemical potentials in liquid and solid has the very large value $\mu_{\text{O Fe}}^{\dagger l} - \mu_{\text{O Fe}}^{\dagger s} = -2.6$ eV, which imples a strong partitioning from solid to liquid. If we repeat our analysis of the outer-core density with the partial molar volume v_{O}^l, we find that an oxygen mole fraction $c_{\text{O}}^l = 0.18$ is needed to match the density of the outer core. Eq. (4) then gives $c_{\text{O}}^s \simeq 0.003$, so that the O concentration in the inner core is very small. With our calculated v_{O}^s value, we then find an ICB density discontinuity of 7.8 ± 0.2 %, which is markedly larger than the seismic value. A binary Fe/O model can thus also be ruled out.

Although all the binary models fail, the seismic data can clearly be accounted for by ternary or quaternary alloys of the three impurities. *Ab initio* calculations on such liquid and solid alloys would certainly be feasible with the methods we have developed, but would need a considerably greater effort. If we assume for the moment that the different impurities do not affect each other's chemical potentials, we can use our present results to construct a model for the core composition. We have seen that S and Si alone cannot explain the density jump at ICB, so there must be some O in the outer core. If we dissolve some O in liquid iron, together with S/Si, maintaining the density of the alloy equal to the density of the core, we increase the density jump at the ICB. This is because hardly any O goes into the solid. We therefore continue to add O till we match the density jump at ICB. The resulting chemical compositions of the inner and outer core are summarized in Table 2.

With these compositions, Eq. (4) now allows us to determine the shift of melting temperature from that of pure Fe at the ICB pressure; we find $\Delta T_m = -700 \pm 100$ K. Comparing this with our earlier *ab initio* melting temperature $T_m = 6200 - 6350$ K for pure Fe at $p = 330$ GPa [18], we obtain the estimate $T_{\text{ICB}} \sim 5600$ K for the temperature at the boundary between inner and outer core. This is quite close to estimates that have been made in other ways [47]. The implications of our temperature and chemical composition results for the understanding of the Earth's dynamics and past history will be explored elsewhere.

6   Discussion and conclusions

We have shown the practical feasibility of calculating completely *ab initio* chemical potentials in liquids and solids, and hence the *ab initio* treatment of chemical equilibrium between co-existing phases. The practical benefits of being able to do such calculations have also been illustrated by showing how they can help to improve our understanding of a controversial and important chemical-equilibrium problem in the earth sciences. We note that, although the calculations are demanding at present because of the need to perform substantial *ab initio* molecular dynamics simulations, the underlying concepts are rather straightforward, and represent a simple extension of well-known classical techniques.

In conclusion, we want to stress that the techniques should have rather wide applications. Although we have chosen to focus on the partitioning of impurities between coexisting solid and liquid phases, the methods could equally well be used to study partitioning between liquid phases, or between solid phases. The ability to calculate *ab initio* chemical potentials in liquids also makes it possible to contemplate the *ab initio* calculation of the solubility of solids, liquids or gases in liquids. The practical application of these ideas is likely to be limited only by the need to find economical thermodynamic integration paths for transforming chemical species into each other.

Acknowledgments

Appendix: from constant volume to constant pressure

We explained in the text that the isobaric dependence of solute chemical potential on concentration is obtained from $(\partial m/\partial c_X)_p$, where m is the non-trivial part of the solute chemical potential, defined in Eq. (16). However, the quantity given by our *ab initio* calculations is $(\partial m/\partial c_X)_V$. We derive here the relation between the isobaric and isochoric derivatives of m.

We start by noting that:

$$
\begin{aligned}
(\partial m/\partial c_X)_p &= (\partial m/\partial c_X)_V + (\partial m/\partial V)_{c_X}(\partial V/\partial c_X)_p \\
&= (\partial m/\partial c_X)_V + (\partial m/\partial V)_{c_X} N(v_X - v_A) ,
\end{aligned} \tag{A1}
$$

with T held constant throughout, where N is the total number of atoms, and we have used the basic definition of the partial molar volumes v_X and v_A of solute and solvent. Next, we refer to Eq. (15) to see that:

$$
(\partial m/\partial V)_{c_X} = (\partial(\mu_X - \mu_A)/\partial V)_{c_X} , \tag{A2}
$$

which can be reexpressed as:

$$
(\partial m/\partial V)_{c_X} = (\partial(\mu_X - \mu_A)/\partial p)_{c_X}(\partial p/\partial V)_{c_X} = -(v_X - v_A)B_T/V , \tag{A3}
$$

with B_T the isothermal bulk modulus, and we have used the relations $(\partial \mu_X/\partial p)_{c_X} = v_X$ and $(\partial \mu_A/\partial p)_{c_A} = v_A$. Combining Eqs. (A1) and (A3), we have:

$$
(\partial m/\partial c_X)_p = (\partial m/\partial c_X)_V - nB_T(v_X - v_A)^2 , \tag{A4}
$$

where $n = N/V$ is the overall atomic number density.

References

[1] P. Hohenberg and W. Kohn, Phys. Rev. **136**, B864 (1964); W. Kohn and L. Sham, Phys. Rev. **140**, A1133 (1965); R. O. Jones and O. Gunnarsson, Rev. Mod. Phys. **61**, 689 (1989); M. C. Payne, M. P. Teter, D. C. Allan, T. A. Arias, and J. D. Joannopoulos, Rev. Mod. Phys. **64**, 1045 (1992); M. J. Gillan, Contemp. Phys. **38**, 115 (1997); R. G. Parr and W. Yang, *Density-Functional Theory of Atoms and Molecules*, (Oxford University Press, Oxford, 1989).

[2] S. Baroni, P. Giannozzi, and A. Testa, Phys. Rev. Lett. **58**, 1861 (1987).

[3] B. B. Karki, R. M. Wentzcovitch, S. de Gironcoli, and S. Baroni, Phys. Rev. B **62**, 14750 (2000).

[4] A. I. Lichtenstein, R. O. Jones, S. de Gironcoli, and S. Baroni, Phys. Rev. B **62**, 11487 (2000).

[5] J. J. Xie, S. P. Chen, J. S. Tse, S. de Gironcoli, and S. Baroni, Phys. Rev. B, **60**, 9444 (1999).

[6] J. J. Xie, S. de Gironcoli, S. Baroni, and M. Scheffler, Phys. Rev. B, **59**, 965 (1999).

[7] M. Lazzeri and S. de Gironcoli, Phys. Rev. Lett. **81**, 2096 (1998).

[8] N. E. Christensen, Phys. Stat. Sol. B **220**, 325 (2000).

[9] D. Alfè, G. D. Price, and M. J. Gillan, Phys. Rev. B **64**, 045123 (2001).

[10] P. Pavone, S. de Gironcoli, and S. Baroni, Phys. Rev. B **57**, 10421 (1998).

[11] G. Kern, G. Kresse, and J. Hafner, Phys. Rev. B **59**, 8551 (1999).

[12] K. Gaal-Nagy, A. Bauer, M. Schmitt, K. Karch, P. Pavone, and D. Strauch, Phys. Stat. Sol. B **221**, 275 (1999).

[13] N. E. Christensen, D. J. Boers, J. L. van Velsen, and D. L. Novikov, J. Phys. Cond. Matt. **12**, 3293 (2000).

[14] R. Car and M. Parrinello, Phys. Rev. Lett. **55**, 2471 (1985).

[15] O. Sugino and R. Car, Phys. Rev. Lett. **74**, 1823 (1995).

[16] G. A. de Wijs, G. Kresse, and M. J. Gillan, Phys. Rev. B **57**, 8223 (1998).

[17] D. Alfè, M. J. Gillan, and G. D. Price, Nature **401**, 462 (1999).

[18] D. Alfè, M. J. Gillan, and G. D. Price, Phys. Rev. B, submitted. Preprint available in electronic form at http://arXiv.org/ps/cond-mat/0107307.

[19] L. Vočadlo and D. Alfè, Phys. Rev. B, submitted. Preprint available in electronic form at http://arXiv.org/ps/cond-mat/0108460.

[20] B. J. Jesson and P. A. Madden, J. Chem. Phys. **113** 5924 (2000).

[21] E. Smargiassi and R. Car, Phys. Rev. B **53**, 9760 (1996).

[22] E. Smargiassi and P. A. Madden, Phys. Rev. B **51**, 117 (1995).

[23] J. W. Arthur and A. D. J. Haymet, J. Chem. Phys. **109**, 7991 (1998).

[24] F. Birch, J. Geophys. Res. **69**, 4377 (1964).

[25] A. E. Ringwood, Geochem. J. **11**, 111 (1977).

[26] J.-P. Poirier, Phys. Earth Planet. Inter. **85**, 319 (1994).

[27] D. Alfè, M. J. Gillan, and G. D. Price, Nature **405** 172 (2000).

[28] A. Laio, S. Bernard, G. L. Chiarotti, S. Scandolo, and E. Tosatti, Science **287**, 1027 (2000).

[29] P. Shearer and G. Masters, Geophys. J. Int. **102**, 491 (1990); T. G. Masters and P. M. Shearer, J. Geophys. Res. **95**, 21691 (1990).

[30] A. M. Dziewonski and D. L. Anderson, Phys. Earth Planet. Inter. **25**, 297 (1981).

[31] D. Alfè, M. J. Gillan, and G. D. Price, Geophys. Res. Lett. **27**, 2417 (2000).

[32] D. Alfè, M. J. Gillan, and G. D. Price, Earth Planet. Sci. Lett., submitted.

[33] D. Frenkel and B. Smit, *Understanding Molecular Simulation*, Ch. 4 (Academic, New York, 1996).

[34] G. Kresse, J. Furthmüller and J. Hafner, Europhys. Lett. **32**, 729 (1995).

[35] Program available at `http://chianti.geol.ucl.ac.uk/~dario`

[36] L. Stixrude, R. E. Cohen, and D. J. Singh, Phys. Rev. B, **50**, 6442 (1994).

[37] P. Söderlind, J. A. Moriarty, and J. M. Wills, Phys. Rev. B **53**, 14063 (1996).

[38] G. A. de Wijs, G. Kresse, L. Vočadlo, D. Dobson, D. Alfè, M. J. Gillan, and G. D. Price, Nature **392**, 805–807 (1998).

[39] D. Alfè, G. Kresse, and M. J. Gillan, Phys. Rev. B **61**, 132 (2000).

[40] D. Alfè and M. J. Gillan, Phys. Rev. B **58**, 8248 (1998).

[41] D. Alfè, G. D. Price, and M. J. Gillan, Phys. Earth Planet. Inter. **110**, 191 (1999).

[42] J. P. Perdew, J. A. Chevary, S. H. Vosko, K. A. Jackson, M. R. Pederson, D. J. Singh, and C. Fiolhais, Phys. Rev. B **46**, 6671 (1992).

[43] H. K. Mao, J. Xu, V. V. Struzhkin, J. Shu, R. J. Hemley, L. Vočadlo, D. Alfè, G. D. Price, M. J. Gillan, W. Sturham, M. Y. Hu, E. E. Alp, M. Schwoerer-Böhning, D, Häusermann, P. Eng, G. Shen, H. Giefers, R. Lübbers, and G. Wörtmann, Science **292**, 914 (2001).

[44] D. Vanderbilt, Phys. Rev. B **41**, 7892 (1990).

[45] G. Kresse and J. Furthmüller, Phys. Rev. B **54**, 11169 (1996); G. Kresse and J. Furthmüller, Comput. Mater. Sci. **6**, 15 (1996); a discussion of the ultra-soft pseudopotentials used in the VASP code is given in G. Kresse and J. Hafner, J. Phys. Condens. Matter **6**, 8245 (1994).

[46] D. Alfè, Computer Phys. Commun. **118**, 31 (1999).

[47] O. L. Anderson and A. Duba, J. Geophys. Res. **102**, 22659 (1997).

[48] L. Vočadlo, D. Alfè, J. P. Brodholt, G. D. Price, and M. J. Gillan, Phys. Earth Planet. Inter. **117**, 123 (2000).

[49] H. J. Monkhorst and J. D. Pack, Phys. Rev. B **13**, 5188 (1976).

Solute	S	Si	O
$\mu_{XA}^{\dagger l}$	3.5 ± 0.05	2.35 ± 0.02	-6.25 ± 0.2
b_X^l	3.13	1.86	5.6
v_{XA}^l	-0.32	-0.32	-2.72
λ_X^l	6.15	3.6	3.25
$\mu_{XA}^{\dagger s}$	3.75 ± 0.05	2.40 ± 0.02	-3.65 ± 0.2
b_X^s	3.0	1.4	
v_{XA}^s	-0.32	-0.32	-2.35
λ_X^s	5.9	2.7	
$\mu_{XA}^{\dagger l} - \mu_{XA}^{\dagger s}$	-0.25 ± 0.04	-0.05 ± 0.02	-2.6 ± 0.2

Table 1: Calculated chemical potentials (eV units) and partial atomic volumes v_X (Å^3 units) of solutes X = S, Si and O in liquid and h.c.p. solid Fe at conditions close to those of the Earth's core (see text). Chemical potential of X is represented at low mole fraction c_X by $\mu_X = k_B T \ln c_X + \tilde{\mu}_X$, with $\tilde{\mu}_X$ linearized as $\tilde{\mu}_X \simeq \mu_X^{\dagger} + \lambda_X c_X$. The quantity $\mu_{XA}^{\dagger}$ is $\mu_X^{\dagger} - \mu_{Fe}^0$, with μ_{Fe}^0 the chemical potential of pure solvent Fe; v_{XA} is $v_X - v_{Fe}$, with v_{Fe} the volume per atom in pure Fe. The meaning of the calculated quantity b_X used to obtain λ_X is explained in Sec. 4.1. Superscripts l and s indicate liquid and solid.

	Solid	Liquid
Sulfur/Silicon	8.5 ± 2.5	10 ± 2.5
Oxygen	0.2 ± 0.1	8.0 ± 2.5

Table 2: Estimated molar percentages of sulfur, silicon and oxygen in the Earth's solid inner core and liquid outer core obtained by combining *ab initio* calculations and seismic data. Sulfur/silicon entries refer to total percentages of sulfur and/or silicon.
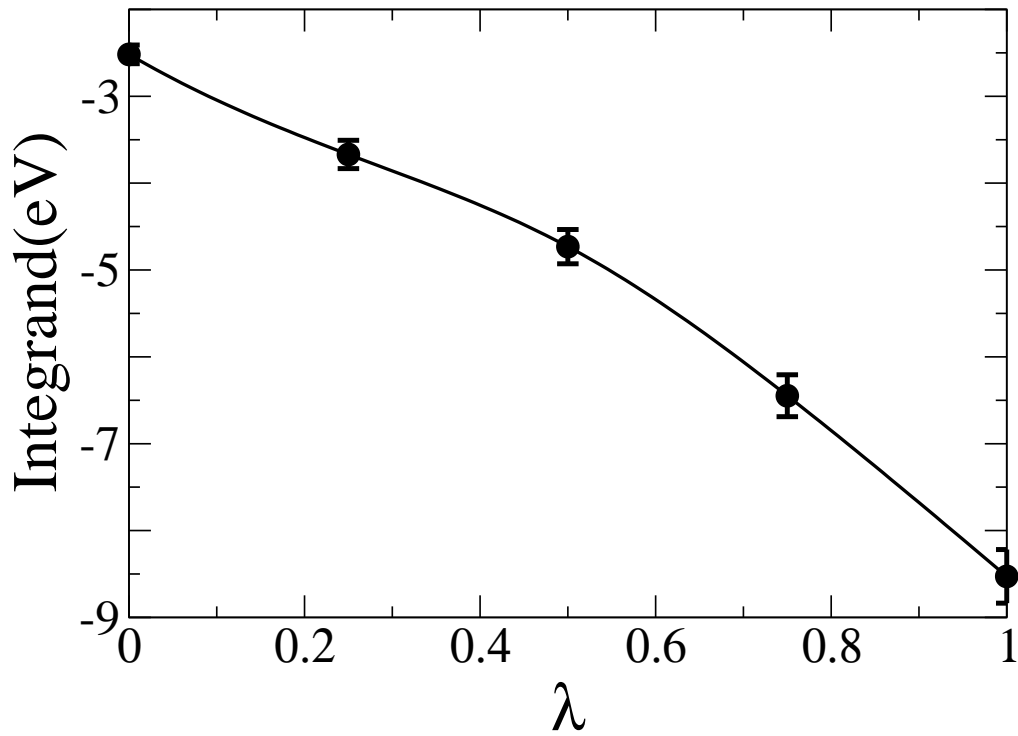
Figure 1: The integrand $\langle U_1 - U_0 \rangle_\lambda$ (eV units) appearing in the thermodynamic integration used to calculate the free energy change $W(N, N_X)$ when N_X atoms of pure solvent are converted into solute atoms, with total number of atoms in the system $= N$ (see Eq. (23)). Results shown refer to oxygen solute for $N_X = 12$ and $N = 64$. Filled circles show values computed from *ab initio* m.d. simulations, with bars indicating statistical errors. Curve is a polynomial fit to the computed values.
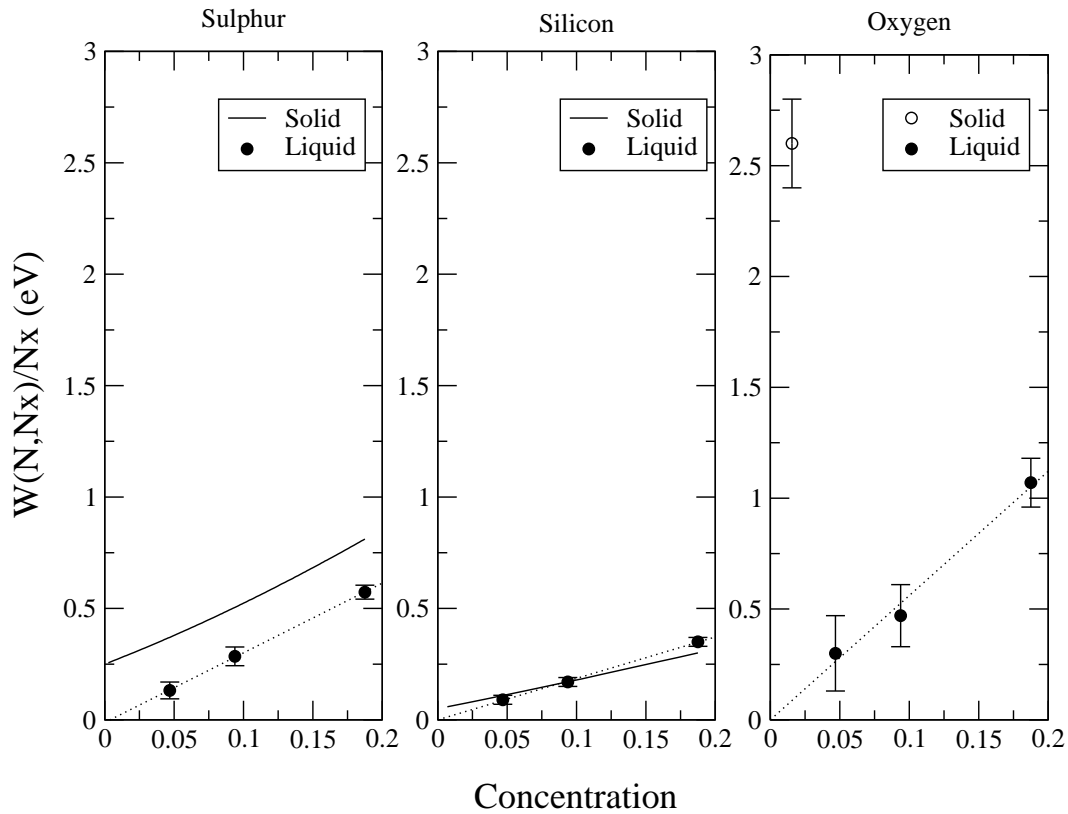
Figure 2: The calculated free energy change $W(N, N_X)$ when N_X atoms of pure solvent are converted into solute atoms, with total number of atoms in the system $= N$. Quantity plotted is $W(N, N_X)/N_X$ (eV units) as a function of concentration $c_X = N_X/N$ for liquid and solid solutions of S, Si and O in Fe. Filled circles are results for liquid, with bars indicating statistical errors, and straight dotted line being a least-squares fit to these data. Continuous curves for S and Si show results for solid solution obtained from Monte Carlo calculations based on *ab initio* free energy of nearest-neighbor interaction. Open circle with error bar is result for O in solid from thermodynamic integration.